The CRISPR Journal
Volume 5, Number 6, 2022

DOI: 10.1089/crispr.2022.0065

The CRISPR Journal

RESEARCH ARTICLE

Bio-Orthogonal Chemistry Conjugation Strategy Facilitates Investigation of N-methyladenosine and Thiouridine Guide RNA Modifications on CRISPR Activity

Alyssa Hoy,† Ya Ying Zheng,† Jia Sheng,* and Maksim Royzen*

Abstract

The CRISPR-Cas9 system is an important genome editing tool that holds enormous potential toward the treatment of human genetic diseases. Clinical success of CRISPR technology is dependent on the incorporation of modifications into the single-guide RNA (sgRNA). However, chemical synthesis of modified sgRNAs, which are over 100 nucleotides in length, is difficult and low-yielding. We developed a conjugation strategy that utilized bio-orthogonal chemistry to efficiently assemble functional sgRNAs containing nucleobase modifications. The described approach entails the chemical synthesis of two shorter RNA oligonucleotides: a 31-mer containing tetrazine (Tz) group and a 70-mer modified with a *trans*-cyclooctene (TCO) moiety. The two oligonucleotides were conjugated to form functional sgRNAs. The two-component conjugation methodology was utilized to synthesize a library of sgRNAs containing nucleobase modifications such as N^1-methyladenosine (m^1A), N^6-methyladenosine (m^6A), 2-thiouridine (s^2U), and 4-thiouridine (s^4U). The impact of these RNA modifications on overall CRISPR activity were investigated *in vitro* and in Cas9-expressing HEK293T cells.

Introduction

The CRISPR-Cas9 system is a powerful genome editing tool that profoundly revolutionized biomedical research and holds enormous potential for successful treatment of human genetic diseases. The two-component system, consisting of a single-guide RNA (sgRNA) and a DNA nuclease, Cas9, forms a complex that is capable of targeting double-stranded DNA with single nucleotide precision.[1,2] This technology has been successfully applied for genome editing at the cellular level,[3,4] as well as *in vivo*.[5–7] In recent years, CRISPR technology has been evaluated in several human clinical trials for the treatment of blood disorders,[8] various cancers,[9–11] eye disease,[12] and chronic infection.[13]

Virtually all FDA-approved RNA-based therapeutics contain RNA modifications.[14–17] The clinical success of CRISPR technology is likely dependent on well-designed incorporation of RNA modifications that can potentially improve sgRNA stability, on-target efficiency and lower off-target effects. A number of RNA modifications have already been explored to achieve these goals.[18–21] None of the reported systems, however, examined sgRNA containing nucleobase modifications, which are common in nature and capable of regulating critical cellular processes.[22]

This is likely due to the fact that sgRNA is over 100-nt long, and solid phase synthesis (SPS) of long oligonucleotides is difficult. Further, the incorporation of nucleobase-modified RNA phosphoramidites during SPS exacerbates the problem, as it is typically associated with lower coupling yields. Our goal has been to develop a versatile synthetic approach that will allow to examine the effects of modified nucleobases such as N^1-methyladenosine (m^1A), N^6-methyladenosine (m^6A), 2-thiouridine (s^2U), and 4-thiouridine (s^4U) on CRISPR activity.

We were inspired by the recently reported ''split-and-click'' strategy, illustrated in Figure 1A, which utilizes copper-catalyzed azide alkyne cycloaddition (CuAAC) chemistry to form functional sgRNAs from two smaller oligonucleotide fragments.[23] This approach entails

Department of Chemistry, University at Albany, SUNY, Albany, New York, USA.
†*Both these authors are co-first authors.*

*Address correspondence to: *Jia Sheng, Department of Chemistry, University at Albany, SUNY, 1400 Washington Ave., Albany, NY 12222, USA,* E-mail: jsheng@albany.edu or *Maksim Royzen, Department of Chemistry, University at Albany, SUNY, 1400 Washington Ave., Albany, NY 12222, USA,* E-mail: mroyzen@albany.edu

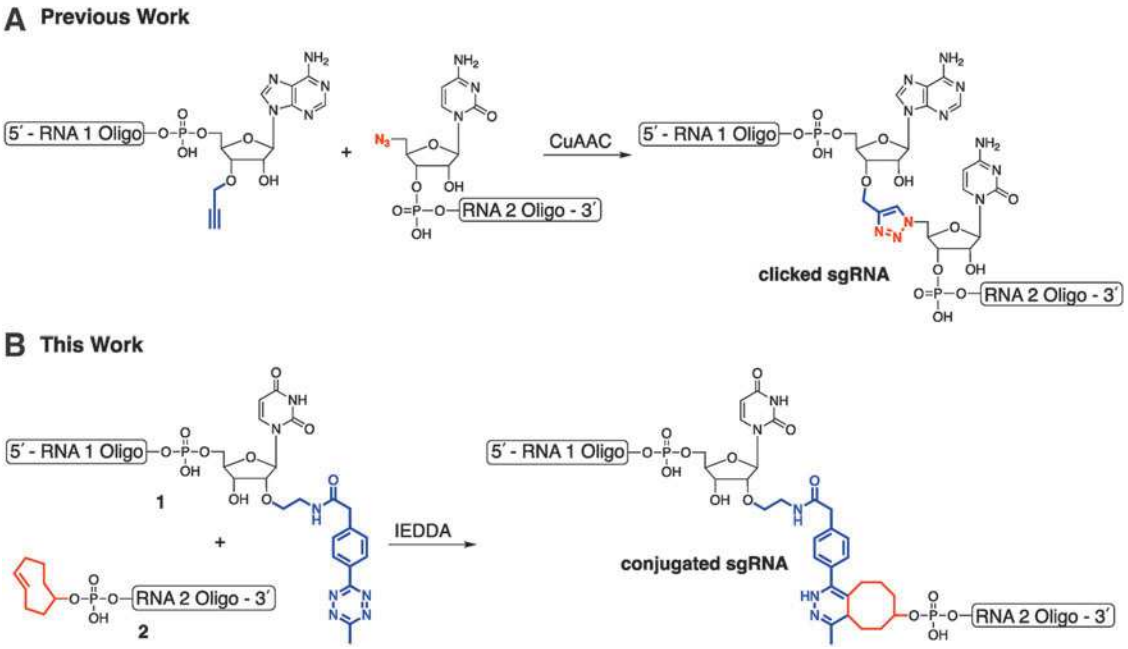

FIG. 1. **(A)** Previously reported "split-and-click" approach to form functional sgRNAs using CuAAC chemistry. **(B)** Synthesis of conjugated sgRNAs using IEDDA chemistry. CuAAC, copper-catalyzed azide alkyne cycloaddition; IEDDA, inverse electron demand Diels-Alder; sgRNA, single-guide RNA.

modification of the 3′-end of RNA 1 oligonucleotide with an alkyne group and modification of the 5′-end of RNA 2 oligonucleotide with an azide group. The two reacting groups are small, and the resulting triazole linker has been shown to cause minimal structural perturbation to ''clicked'' sgRNAs.

One of the drawbacks of the reported approach is that the ligation chemistry is catalyzed by Cu(I), which is biologically toxic and should ideally be avoided in the synthesis of therapeutic RNAs.[24] Our goal was to investigate whether the ''split-and-click'' strategy could be successfully accomplished using inverse electron demand Diels-Alder (IEDDA) chemistry, which does not require Cu(I) catalysis. The bio-orthogonal IEDDA chemistry has been shown to be compatible with the intricate functional groups and structural elements of RNA.[25–27]

As illustrated in Figure 1B, our approach entails modification of the 2′-end of RNA 1 oligonucleotide with a tetrazine (Tz) group and modification of the 5′-end of RNA 2 oligonucleotide with a *trans*-cyclooctene (TCO) moiety. The two oligonucleotides can be conjugated in a biological buffer under neutral pH and without any transition metal catalyst, thus forming ''conjugated'' sgRNA (Fig. 1B). Watts and co-workers recently reported a similar bioconjugation strategy bridging two segments of sgRNA in the tetraloop region using Tz and norbornene.[28]

Materials and Methods

All oligonucleotide solid phase syntheses were done on a 1.0 μmol scale using the Oligo-800 synthesizer (Azco Biotech, Oceanside, CA). Solid phase syntheses were performed on controlled pore glass. (CPG-1000) purchased from Glen Research (Sterling, VA). Other oligonucleotide SPS reagents were obtained from ChemGenes Corporation (Wilmington, MA). Phosphoramidites (TBDMS as the 2′-OH protecting group): rA was N-Bz protected, rC was N-Ac protected, and rG was N-iBu protected. A, C, G, and U phosphoramidites were dissolved in anhydrous acetonitrile (0.07 M) directly before use. m^1A, m^6A, s^2U, and s^4U phosphoramidites were dissolved in anhydrous acetonitrile (0.15 M) directly before use.

A coupling step was done using 5-ethylthio-1H-tetrazole solution (0.25 M) in acetonitrile for 12 min. 5′-Detritylation step was done using 3% trichloroacetic acid in CH_2Cl_2. Oxidation step was done using I_2 (0.02 M) in THF/pyridine/H_2O solution. The CPG modifications were carried out using native amino lcaa CPG 1000 Å, purchased from ChemGenes Corporation (Cat. No. N-5100-10).

For gel electrophoresis, 10 × Tris/Borate/EDTA (TBE) buffer was purchased from Fisher Scientific Company, LLC (Waltham, MA) and used with proper dilution. Thirty percent Arcylamide/Bis-arcylamide solution (29:1) was purchased from Bio-Rad Laboratories, Inc.

(Hercules, CA). Chromatographic purifications of synthetic materials were conducted using SiliaSphere™ spherical silica gel with an average particle and a pore size of 5 μm and 60 Å, respectively (Silicycle, Inc., Quebec, Canada). Thin layer chromatography (TLC) was performed on SiliaPlate™ silica gel TLC plates with 250 μm thickness (Silicycle, Inc.).

Flash chromatography was performed using Biotage Isolara One instrument (Biotage Sweden AB, Uppsala, Sweden). Preparative TLC was performed using SiliaPlate silica gel TLC plates with 1000 μm thickness. ^{1}H, ^{13}C, and ^{31}P nuclear magnetic resonance (NMR) spectroscopy was performed on a Bruker NMR at 500 MHz (^{1}H) and 126 MHz (^{13}C) and 121 MHz (^{31}P). All ^{13}C NMR spectra were proton decoupled. High-resolution electrospray ionization–mass spectrometry (ESI-MS) spectra of small molecules was acquired using Agilent Technologies 6530 Q-TOF instrument. The ESI-MS analysis of RNA oligonucleotides was carried out by Novatia, LLC (Newtown, PA).

Synthesis of RNA oligonucleotides containing TCO

The phosphoramidite **7**, containing TCO, was coupled during the final synthetic cycle of SPS of RNA. The subsequent oxidation step was performed using 1 M solution of t-BuOOH in CH_2Cl_2. After completion of SPS, CPG beads were treated with concentrated aqueous ammonia in a sealed vial for 2 h at 55°C. The ammonia was removed in vacuo (SpeedVac). Cleaved oligonucleotides were redissolved in mixture of anhydrous DMSO (100 μL) and triethylamine trihydrofluoride (125 μL) and heated for 2.5 h at 65°C.

After subsequent cooling to room temperature (rt), sodium acetate buffer (3 M, pH 5.2, 25 μL) and ethanol (1 mL) were added, and the RNA was stored overnight at −20°C. The RNA was then pelleted by centrifugation (14,000 *g*, 17 min, 4°C), the supernatant was discarded, and the pellet was washed with 75% ethanol (1 mL). The pellet was then dried in vacuo, and it was dissolved in water.

Assessment of TCO coupling to RNA oligonucleotides

The CPG beads containing RNA 2 oligo-TCO (5 mg) were mixed with Tz-DMT for 1 h at rt. Synthesis of Tz-DMT was previously described (He et al[25]). After the reaction, the beads were thoroughly washed with DMF and CH_2Cl_2. The CPG beads were treated with 10 mL deblocking solution (3% trichloroacetic acid in CH_2Cl_2). Absorbance at 504 nm was used to calculate the amount of cleaved DMT group ($\varepsilon = 76\,mL\cdot cm^{-1}\cdot\mu mol^{-1}$). The amount of coupled TCO was calculated based on the assumption of nearly quantitative reaction between RNA 2 oligo-TCO and Tz-DMT.

Purification of RNA oligonucleotides by preparative polyacrylamide gel electrophoresis

Oligonucleotides were mixed with formamide dye (50% v/v) and loaded onto a denaturing 10–20% polyacrylamide gel (1 × TBE buffer containing 8 M urea) and separated at 500 V for 1–2 h. The RNA bands were visualized under ultraviolet, excised, crushed, and soaked in buffer [ammonium acetate 500 mM, $Mg(OAc)_2$ 10 mM, EDTA 2 mM) 800 μL] for 16 h at rt with vigorous shaking. Buffer volume was reduced to 50 μL by butanol extraction (5 × 500 μL). Cold ethanol (1000 μL) was added, and RNA was precipitated at −20°C overnight.

Cas9 *in vitro* cleavage assay

pBR322 plasmid DNA (0.35 μM, 1.13 μL, N3033S; NEB) was diluted with water (16.87 μL) and NEB buffer 3.1 (10×, 2 μL). The plasmid was linearized directly before CRISPR experiments using PvuII (10 U/μL, 1 μL, R0151S; NEB) for 1 h at 37°C. In analogous fashion, eGFP-N1 plasmid was linearized with DraIII-HF (10 U/μL, 1 μL, R3510L; NEB). For the Cas9-mediated DNA cleavage assay, sgRNA (300 nM, 5 μL), Cas9 (1 μM, 0.3 μL, M0386S; NEB), Cas9 buffer (10×, 1 μL; NEB), linearized plasmid (20 nM, 1.5 μL), and H_2O (2.2 μL) were mixed together (final volume = 10 μL) and incubated for either 1 or 16 h at 37°C.

CRISPR experiments were terminated by the addition of proteinase K (20 mg/mL, 0.5 μL) for 1 h at 37°C. The reaction (1 μL) was mixed with blue loading buffer (6×, 2 μL, B7703S; NEB) and loaded on a 1% agarose stained with ethidium bromide (1 × TBE running buffer).

Evaluation of in-cell CRISPR activity

CRISPR-Cas9 experiments were carried out following the procedure reported by Yin et al.[20] HEK293T cells were infected by lentiviral particles to stably express EF1a-GFP-PGK-Puro (26777; Addgene) and EFs-spCas9-Blast (52962; Addgene). The cells were grown to 70–90% confluence in Dulbecco's modified Eagle's medium (DMEM), containing 10% fetal bovine serum (FBS). The cells were transfected with GFP-targeting sgRNAs (30 nM each, final concentration) using Lipofectamine (Thermo Fisher Scientific) for 24 h. The cells were further grown in DMEM for 48 h post-transfection.

The cells were fixed with 2% paraformaldehyde in PBS, and GFP expression was analyzed by flow cytometry. Data from 10^6 cells were acquired using a FACS Aria III cell sorter equipped with a 488 nm/blue coherent sapphire solid-state laser, 20 mW (BD Biosciences, San Jose, CA). Data analyses were carried out using FlowJo software (Ashland, OR), according to the manufacturer's

instructions. Parameters, such as median fluorescence intensity (MFI) and the percentages of specific populations, were quantified by histogram analysis.

Synthesis of conjugated sgRNA using IEDDA chemistry

RNA 1 oligo **1** containing Tz (250 μmol) and RNA 2 oligo **2** containing TCO (120 μmol) were mixed in an NaCl solution (0.2 M, 7.9 μL), containing EDTA (0.5 M, 0.2 μL) and HEPES (0.2 M, pH 7.5, 2 μL). The reaction mixture was agitated at 1000 rpm at rt for 16 h. The conjugated sgRNA was purified by preparative PAGE.

Results

The synthesis of the two RNA components described in our strategy for making conjugated sgRNA is illustrated in Figure 2. Toward attachment of Tz to the 2′-end of RNA 1 oligonucleotide, we synthesized controlled pore glass (CPG) solid support **3** that was modified with a uridine analog containing trifluoroacetyl-protected amine group at the 2′-position.[29,30] After completion of the SPS of RNA and subsequent cleavage, deprotection, and desilylation steps, the resulting RNA 1 oligonucleotide will contain an amine group that was coupled to the Tz-NHS ester **5**. Our choice of Tz was based on the reports that indicated its exceptional stability under physiological conditions.[31,32]

The Tz-modified RNA oligonucleotides were purified by preparative PAGE and characterized by ESI-MS (Supplementary Figs. S1–S14). As illustrated in Figure 2B, 5′-end of RNA 2 oligonucleotide was modified with TCO using previously reported TCO-phosphoramidite **7**.[33] Compound **7** was incorporated at the final coupling step of SPS. Modified oxidation step (Supplementary Data) using *tert*-butyl hydroperoxide was used due to sensitivity of TCO to the standard SPS oxidation chemistry. The TCO-modified RNA oligonucleotides were obtained after the standard cleavage, deprotection, and desilylation steps.

The conjugated sgRNAs that are formed via IEDDA chemistry contain a linker that is considerably larger than the triazole linker (Fig. 1A). According to experimental analysis described by Taemaitree et al, this could potentially be detrimental for CRISPR activity due to perturbation of native interactions between sgRNA and Cas9.[23] Our goal was to find a site where longer linkers would be well tolerated. We were inspired by Iwasaki et al, who reported sgRNA constructs containing fused theophylline aptamer capable of regulating CRISPR activity.[34]

We synthesized three sgRNAs in which the two RNA segments were conjugated together at different positions in the repeat region, as shown in Figure 3. The conjugated sgRNAs were purified by preparative PAGE, as illustrated in Supplementary Figure S15. The sequence of the constructed sgRNAs has been reported to target linearized pBR322 plasmid.[23]

The constructs described in Figure 3 were tested *in vitro* for their ability to carry out Cas9-mediated cleavage of linearized pBR322 plasmid. All of the CRISPR experiments described here and beyond were carried out in duplicate. As illustrated in Figure 4, **sgRNA 1** and **sgRNA 2** were unable to facilitate DNA cleavage, presumably due to the prohibitively long linker. Fortunately, **sgRNA 3** was found to be active (lanes 6 and 7). In fact, **sgRNA 3** outperformed the unmodified sgRNA (lanes 2 and 3).

These findings proved that placement of the long linker is crucial to facilitate proper RNA-Cas9 interactions that

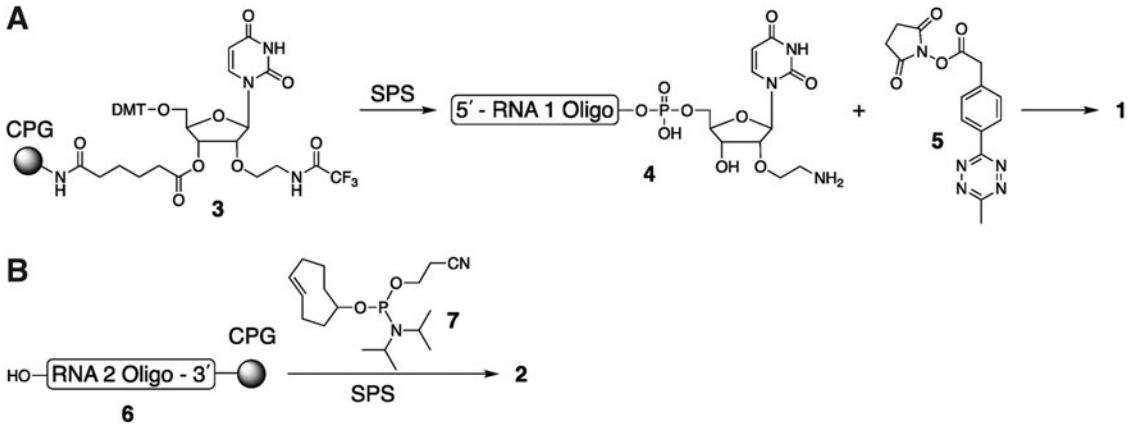

FIG. 2. **(A)** Synthesis of the RNA oligonucleotide-modified with Tz; **(B)** Synthesis of the RNA oligonucleotide-modified with TCO. TCO, *trans*-cyclooctene; Tz, tetrazine.

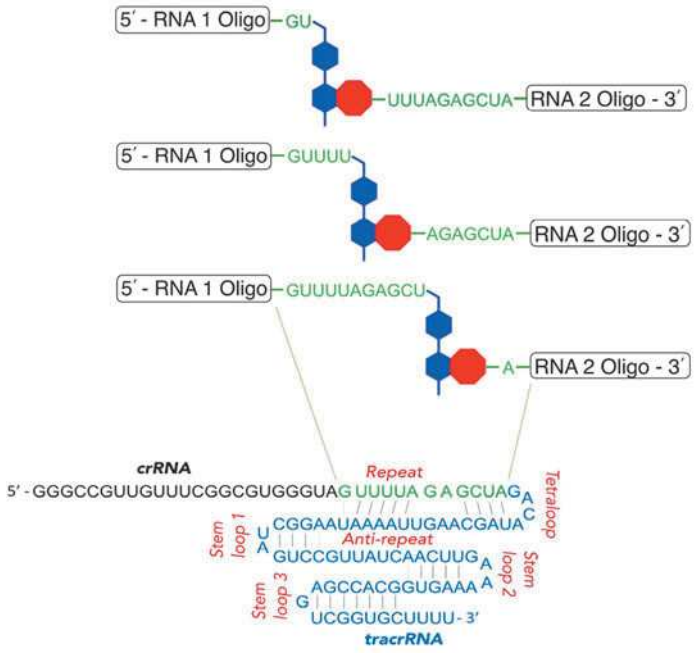

	RNA 1 Oligo	RNA 2 Oligo
sgRNA 1	25mer-Tz	TCO-78mer
sgRNA 2	28mer-Tz	TCO-75mer
sgRNA 3	34mer-Tz	TCO-69mer

FIG. 3. Synthesis of conjugated sgRNA constructs by ligating two RNA fragments using IEDDA chemistry.

enable nuclease activity. To test the generality of our approach, we synthesized **sgRNA 4** targeting the GFP gene encoded on the linearized eGFP-N1 plasmid (Table 1 and Supplementary Table S1). The new construct was linked at the same location in the repeat sequence as **sgRNA 3**. As illustrated in Figure 5A, **sgRNA 4** (lanes 4 and 5) was also found to be active also outperforming the corresponding unmodified sgRNA (lanes 2 and 3).

Empowered by the synthetic methodology to assemble functional conjugated sgRNAs, we turned our attention toward investigation of the effects of nucleobase modifications m^1A, m^6A, s^2U, and s^4U on CRISPR activity. The chosen RNA modifications are known to play important regulatory roles in cellular biochemistry. m^1A has been found in ribosomal RNA (rRNA), transfer RNA (tRNA), and messenger RNA (mRNA).[35–38] When incorporated into mRNA, m^1A can upregulate translation.[36] A single m^1A modification in the vicinity of the start codon resulted in a 1.2–1.4 higher mRNA translation efficiency in both human and mouse cells.[36]

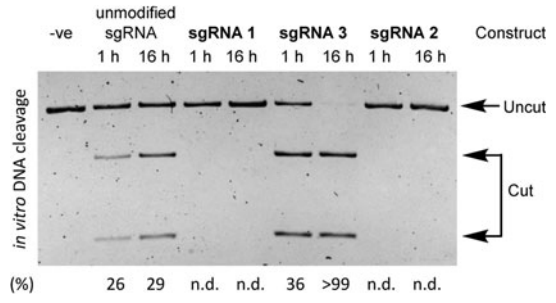

FIG. 4. Activity of unmodified sgRNA, **sgRNA 1**, **sgRNA 2,** and **sgRNA 3** constructs in facilitating Cas9-mediated cleavage of linearized pBR322 plasmid at 1 and 16 h time points.

Similarly, recent transcriptome-wide m^6A-seq studies also discovered m^6A RNA modification in 5′-untranslated region (UTR) and start codons.[39,40] m^6A regulates translation of mRNA by recruiting m^6A reader proteins, such as YTHDF1, YTHDF2, and YTHDF3; as well as YTHDC1 and YTHDC2,[41] which promote mRNA translation. Another recent study reported that m^6A also repels certain RNA-binding proteins, forming an additional layer of regulation of mRNA translation.[42] Meanwhile, s^2U and s^4U are known to be present in certain tRNAs. s^2U has been found at position 34 of tRNA, the first position of the anticodon, which is base-paired with the nucleotide at the wobble position of the mRNA codon.[43]

The presence of s^2U has been attributed to codon-anticodon recognition efficiency and accuracy. The RNA modification has been shown to enhance the aminoacylation kinetics of tRNA, and to prevent frame-shifting during translation.[44]

The aforementioned RNA modifications were incorporated in the CRISPR RNA (crRNA) region (Table 1), which is responsible for the recognition of complementary target DNA.[1,2] Based on previously reported studies, m^1A, m^6A, and s^4U will destabilize RNA-DNA duplex, whereas

Table 1. Sequences of the CRISPR RNA region of GFP-targeting single guide RNAs containing nucleobase modifications

Construct	*Sequence*	*Note*
sgRNA 4	5′-GGG CGA GGA GCU GUU CAC CGG UUU …-3′	Unmodified RNA
sgRNA 5	5′-GGG CGA GGA GC**A** GUU CAC CGG UUU …-3′	One U to A mismatch
sgRNA 6	5′-GGG CGA GGA GC**A** G**AA** CAC CGG UUU …-3′	Three U to A mismatches
sgRNA 7	5′-GGG CG**m^{1}A** GG**m^{1}A** GCU GUU C**m^{1}A**C CGG UUU …-3′	Three **m^{1}A** modifications
sgRNA 8	5′-GGG CG**m^{6}A** GG**m^{6}A** GCU GUU C**m^{6}A**C CGG UUU …-3′	Three **m^{6}A** modifications
sgRNA 9	5′-GGG CGA GGA GC**s^2 UGs^2 Us^{2}U** CAC CGG UUU …-3′	Three **s^{2}U** modifications
sgRNA 10	5′-GGG CGA GGA GC**s^{4}UGs^{4}Us^{4}U** CAC CGG UUU …-3′	Three **s^{4}U** modifications
sgRNA 11	5′-GGG CGA GGA GC**s^{2}U** GUU CAC CGG UUU …-3′	One **s^{2}U** modification
sgRNA 12	5′-GGG CGA GGA GC**s^{2}UGs^{2}U** U CAC CGG UUU …-3′	Two **s^{2}U** modifications
sgRNA 13	5′-GGG CGA GGA GC**s^{4}U** GUU CAC CGG UUU …-3′	One **s^{4}U** modification
sgRNA 14	5′-GGG CGA GGA GC**s^{4}UGs^{4}U** U CAC CGG UUU …-3′	Two **s^{4}U** modifications

m^{1}A, N^1-methyladenosine; m^{6}A, N^6-methyladenosine; s^{2}U, 2-thiouridine; s^{4}U, 4-thiouridine; sgRNA, single-guide RNA.

s^{2}U will have stabilizing effects.[45–47] Our convergent approach facilitated efficient assembly of **sgRNAs 5–10** using the two-component conjugation strategy. The RNA modifications, whose coupling is often associated with lower yields, were incorporated into the shorter, 31-nt long, RNA 1 oligonucleotide (Fig. 1B). **sgRNAs 5–10** share the same 70-nt long RNA 2 oligonucleotide component (Fig. 1B).

First, to get an idea of how many modifications would be necessary to observe a pronounced effect, we synthesized **sgRNA 5** and **sgRNA 6** (Table 1) that contain either one or three U to A mismatches. As illustrated in Figure 5A, a single mismatch in **sgRNA 5** does not have a pronounced impact on the nuclease activity. On the other hand, the incorporation of three U to A mismatches in the **sgRNA 6** rendered it completely inactive. Therefore, to investigate the impacts of RNA modifications, we decided to synthesize **sgRNAs 7**, **8**, **9,** and **10** containing three m^{1}A, m^{6}A, s^{2}U, and s^{4}U modifications, respectively (Table 1).

As illustrated in Figure 5B, the incorporation of three m^{1}A modifications in **sgRNA 7** completely eliminated nuclease activity. This was an expected outcome, as methylation at the 1-position of adenosine disrupts hydrogen bonding to a complimentary thymidine. Consequently, three m^{1}A residues disrupted the ability of **sgRNA 7** to recognize and bind the complimentary double-stranded DNA (dsDNA). Analogous behavior was observed with **sgRNA 10**, which contains three s^{4}U residues. S^{4}U was reported to destabilize the duplex by 0.6 kcal/mol, which was attributed to weaker Watson–Crick base pairing due to the replacement of the hydrogen bond accepting oxygen by a weaker hydrogen bond accepting sulfur at C4.[45]

Meanwhile, quite unexpected results were observed with **sgRNA 8** and **sgRNA 9**. It has been reported that s^{2}U modification leads to increased duplex stability by about 1 kcal/mol.[46,48] The increased stability has been attributed to enhanced stacking interactions and higher acidity of the N-3 proton and thus increased strength of its hydrogen bond.[46,48] However, the incorporation of three s^{2}U residues in **sgRNA 9** led to lower CRISPR activity relative to **sgRNA 4**, which contains canonical nucleobases. On the other hand, **sgRNA 8**, containing three m^{6}A residues exhibited higher nuclease activity than **sgRNA 4**.

This finding was also unexpected, as N^6-methylation is known to have a destabilizing effect in base-paired regions of RNA by 0.5–1.7 kcal/mol. The N^6-methyl group has been predicted to be in a high-energy anti conformation, with the methyl group oriented into the major groove of the RNA, where the amino proton would normally be.[47]

Hoping to find some predictable trends, we decided to further investigate the impacts of s^{2}U and s^{4}U nucleobase modifications on CRISPR activity. We synthesized **sgRNA 11** and **sgRNA 12** that contain one and two s^{2}U modifications, as well as **sgRNA 13** and **sgRNA 14** that contain one and two s^{4}U modifications (Table 1 and Supplementary Table S1). The new constructs were tested for their ability to carry out Cas9-mediated cleavage of linearized eGFP-N1 plasmid and correlated to **sgRNA 9** and **sgRNA 10** that contain three s^{2}U and s^{4}U modifications, respectively. As illustrated in Figure 5C, all of sgRNAs containing s^{2}U RNA modifications exhibited lower nuclease activity than the unmodified **sgRNA 4**, without any noticeable trends.

The **sgRNA 14**, containing two s^{4}U modification, was found to be completely inactive, just like the previously tested **sgRNA 10**. Perhaps, the most interesting result was observed with **sgRNA 13**, which contains a single s^{4}U modification. It was found to have the highest nuclease activity of all the tested modified sgRNAs. All of the described CRISPR experiments are summarized in Figure 5D.

The ability of conjugated sgRNAs, containing m^{6}A and s^{2}U modifications, to enable Cas9 nuclease activity

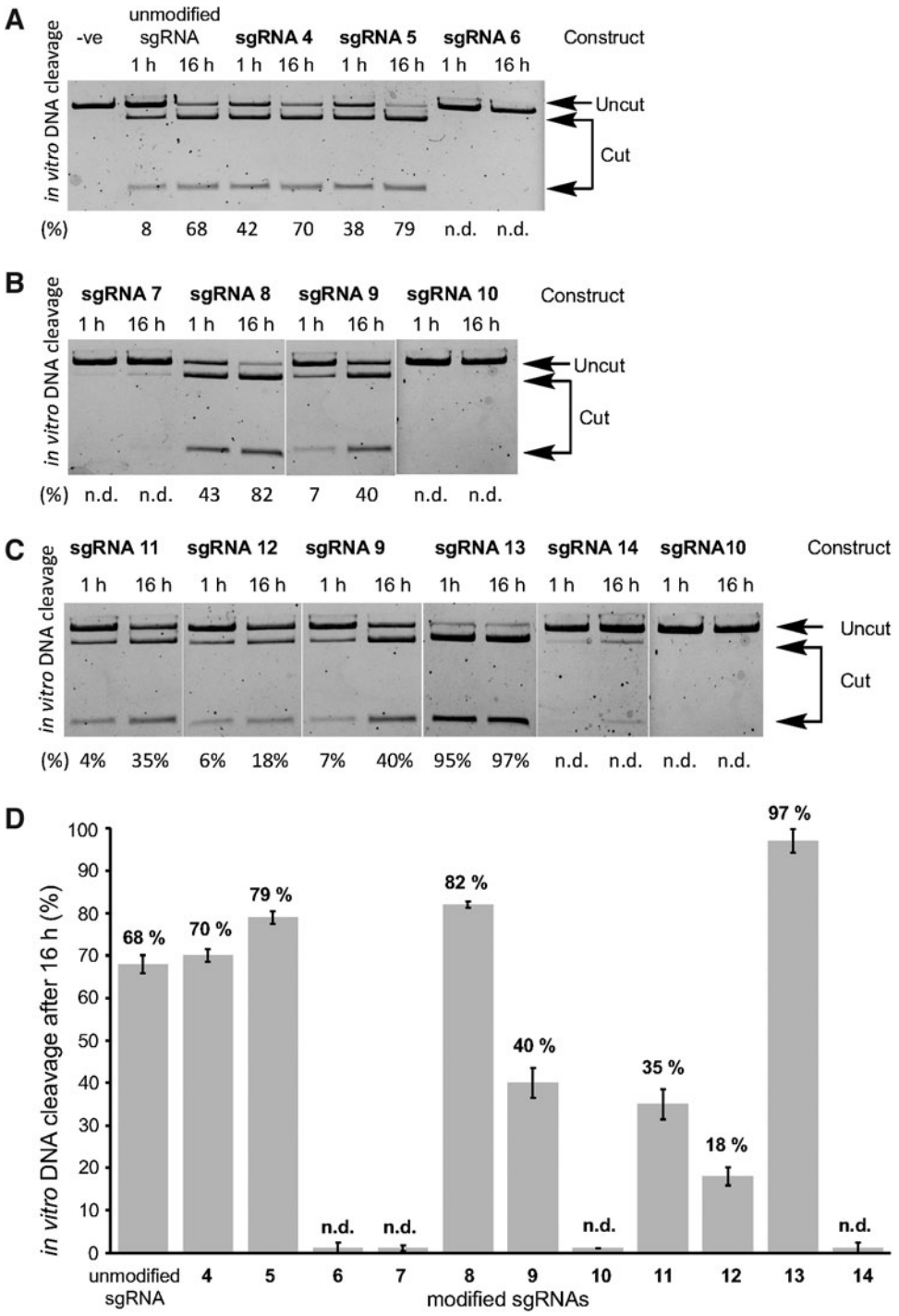

FIG. 5. **(A)** Activity of unmodified sgRNA and **sgRNA 4**, **sgRNA 5,** and **sgRNA 6** constructs in facilitating Cas9-mediated cleavage of linearized eGFP-N1 plasmid at 1 and 16 h time points. All experiments were done in duplicate. **(B)** Activity of sgRNAs containing m^1A, m^6A, s^2U, and s^4U modifications (**sgRNA 7**, **sgRNA 8**, **sgRNA 9,** and **sgRNA 10**) in facilitating Cas9-mediated cleavage of linearized eGFP-N1 plasmid at 1 and 16 h time points. **(C)** Activity of sgRNAs containing one, two, and three s^2U and s^4U modifications (**sgRNA 9**, **sgRNA 10**, **sgRNA 11**, **sgRNA 12**, **sgRNA 13,** and **sgRNA 14**) in facilitating Cas9-mediated cleavage of linearized eGFP-N1 plasmid at 1 and 16 h time points. **(D)** Summary of Cas9-mediated cleavage of linearized eGFP-N1 plasmid after 16 h. m^1A, N^1-methyladenosine; m^6A, N^6-methyladenosine; s^2U, 2-thiouridine; s^4U, 4-thiouridine.

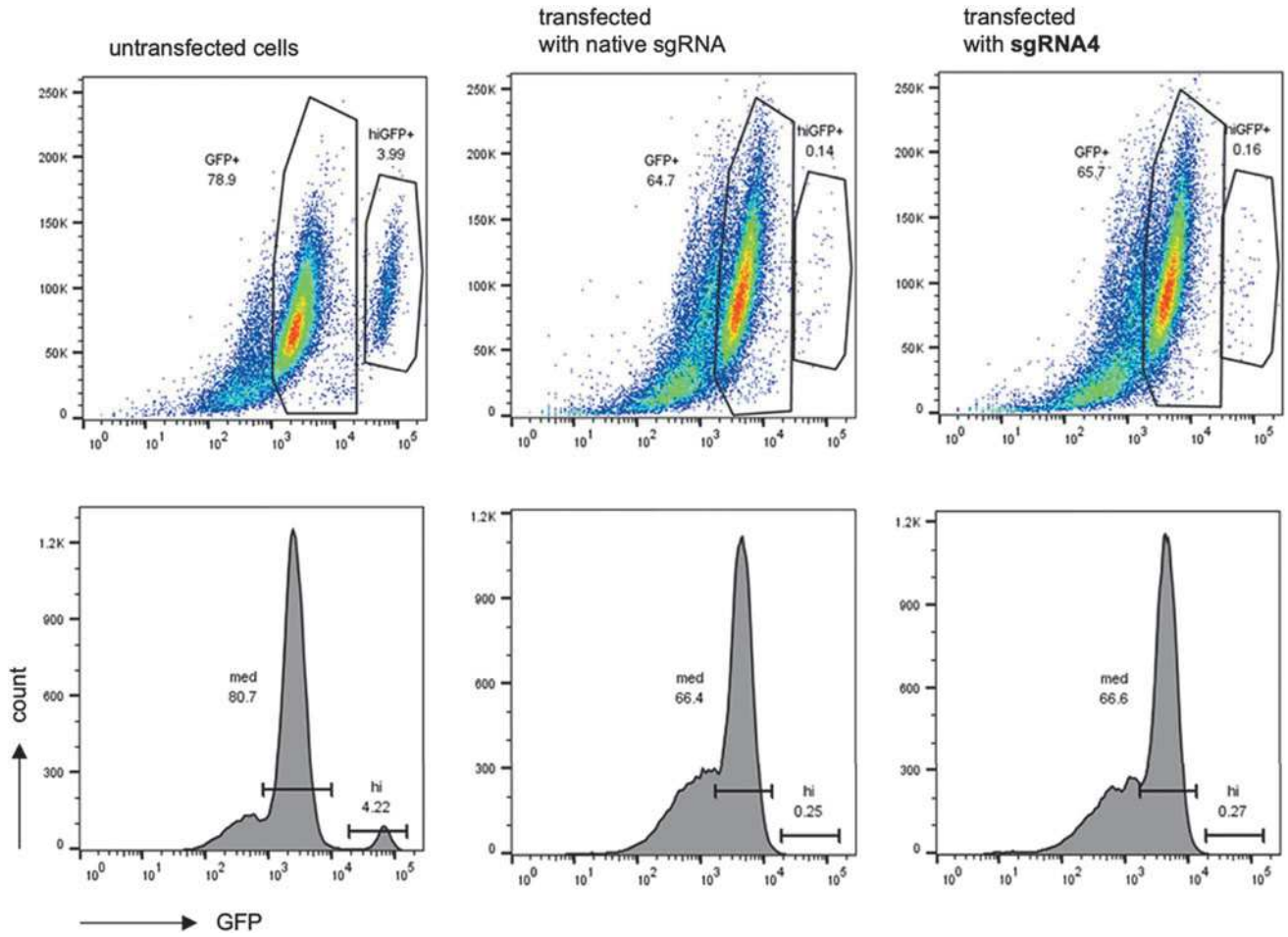

FIG. 6. Flow cytometry analysis of GFP expression of GFP and Cas9-expressing HEK293T transfected with native sgRNA and **sgRNA4**.

was tested in GFP and Cas9-expressing HEK293T cells.[20] The cells were transfected for 24 h with the GFP-targeting **sgRNA 4**, **sgRNA 8,** and **sgRNA 9**, as well as unmodified sgRNA, as a positive control. The cells were analyzed by flow cytometry 48 h post transfection to investigate the expression of GFP. As illustrated in Figure 6, the untransfected cells show two subpopulations of GFP-expressing cells.

The subpopulation with higher GFP fluorescence corresponds to 4.16% ± 0.44% of total cells, whereas the subpopulation with lower GFP signal corresponds to 78.93% ± 0.25% of total cells. Transfection with unmodified sgRNA almost completely eliminated the subpopulation of cells with higher GFP fluorescence (0.25% ± 0.14%), while also decreasing the subpopulation of cells with a lower GFP signal to 66.37% ± 3.69%. Analogous behavior was observed with the cells transfected with **sgRNA 4** (higher GFP subpopulation 0.20% ± 0.05%; lower GFP subpopulation 67.07% ± 1.18%).

This indicated that **sgRNA4** is functional inside the cells to enable nuclease activity that is on par with the native system. Contrary to the prediction from the *in vitro* experiments, **sgRNA 8** and **sgRNA 9** were found to have lower CRISPR activity inside the cells. The flow cytometry analysis illustrated in Figure 7 indicates that the cells transfected with **sgRNA 8** had a higher GFP-expressing subpopulation of 2.12% ± 0.07% and a lower GFP-expressing subpopulation of 74.07% ± 0.60%. Similarly, the cells transfected with **sgRNA 9** had a higher GFP-expressing subpopulation of 2.31% ± 0.11% and a lower GFP-expressing subpopulation of 69.80% ± 0.85%. These data are summarized in Figure 8.

Discussion

The CRISPR-Cas9 system is a powerful genome editing tool whose clinical translation will likely require thorough structural optimization. Cas9-guided nuclease activity is dependent on the interactions between the enzyme and

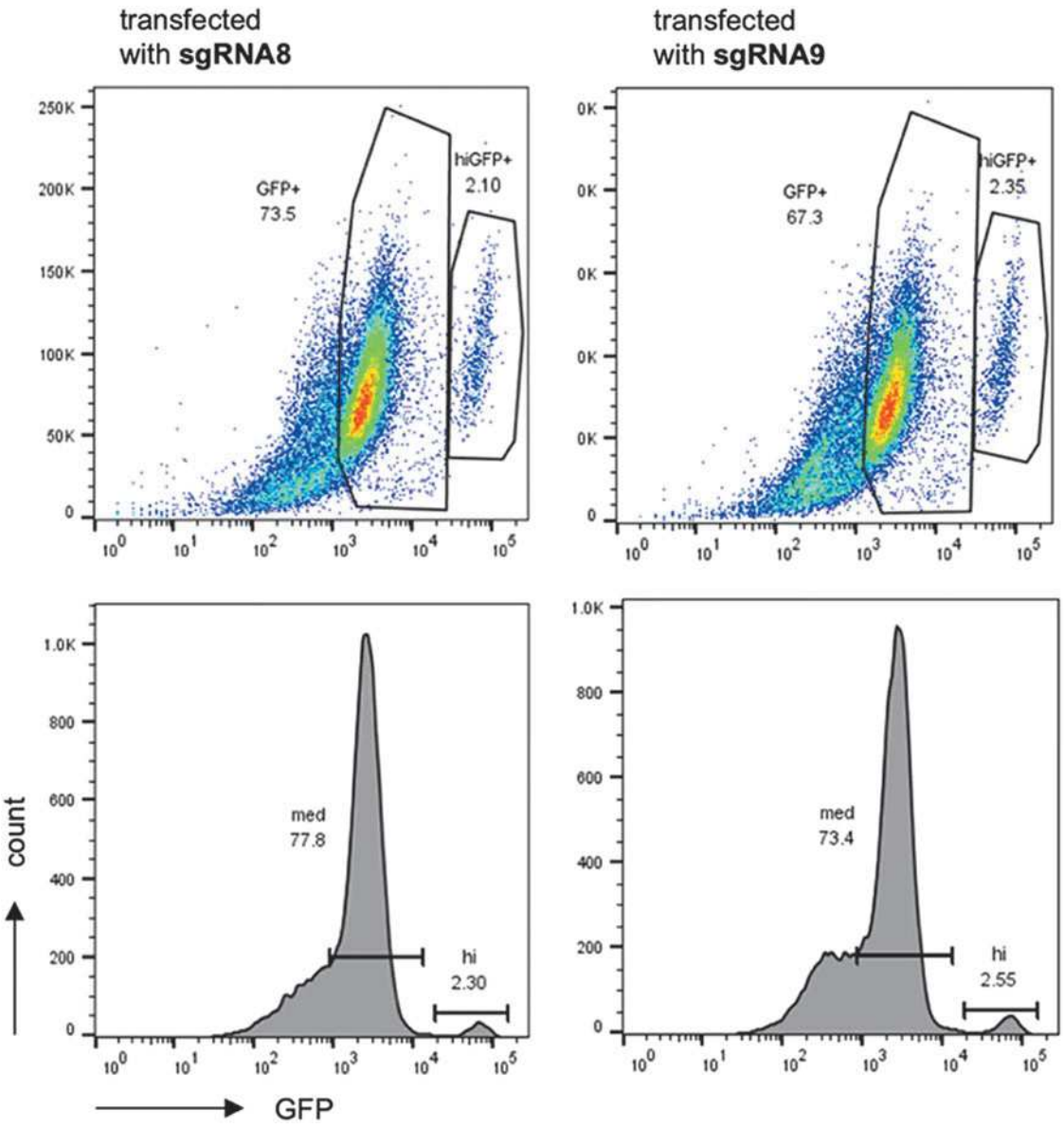

FIG. 7. Flow cytometry analysis of GFP expression of GFP and Cas9-expressing HEK293T transfected with **sgRNA8** and **sgRNA9**.

sgRNA, as well as the subsequent recognition and association between this Cas9-sgRNA complex and target dsDNA. This multi-step process has been demonstrated by structural studies to involve a cascade of conformational changes within the RNA-enzyme-DNA system.[49,50] In recent years, a number of different strategies have evolved to manipulate and optimize each of the three components and improve the overall CRISPR efficiency and specificity of DNA cleavage.

For example, new and improved Cas9 variants have been reported, such as eSpCas9, SpCas9-HF1, and HypaCas9.[51–53] In comparison, the strategy of changing the sequence, stability or conformation of guide RNA requires relatively less effort than new enzyme engineering. Riesenberg et al incorporated highly stable hairpins into guide RNA to ensure proper folding that leads to improved genome editing regardless of spacer sequence composition.[54] It has been shown that chemical modifications on guide RNA such as 2′-deoxy, 2′-F, 2′-O-methyl, locked nucleic acids (LNA), and phosphorothioated backbone can also improve nuclease activity and gene editing efficiency probably due to both enhanced interactions within the CRISPR system and increased biostability of RNA.[18,55–58]

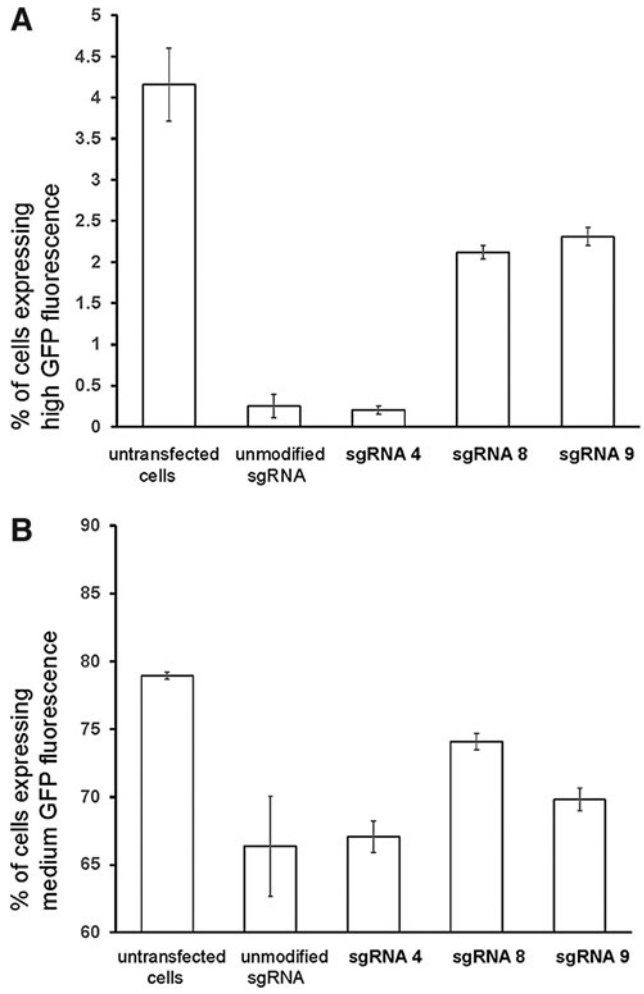

FIG. 8. Flow cytometry analysis of GFP expression of GFP and Cas9-expressing HEK293T transfected with unmodified sgRNA, **sgRNA 4**, **sgRNA8,** and **sgRNA9**. **(A)** Subpopulation of cells with high GFP fluorescence, **(B)** subpopulation of cells with medium GFP fluorescence. All flow cytometry experiments were done in triplicate.

However, balancing and optimizing the Cas9 cleavage efficiency and on-target specificity remains a big challenge for gene editing and requires more systematic investigation. From this perspective, using naturally or artificially modified nucleobases to further adjust the interactions of crRNA, Cas9 and target DNA represents a promising approach. There are many base modifications that are currently available to fine-tune the stability and specificity of RNA binding with both Cas9 and DNA. Due to the intrinsic synthetic challenges of making long base-modified RNA strands, such methods have not been well explored.

Our metal-free IEDDA chemistry-based bio-orthogonal method improves the RNA synthesis yield and facilitates construction of a model platform to thoroughly study the overall DNA cleavage effects of all the base modifications with available phosphoramidite building blocks.

In the current work, we demonstrated that the TCO-Tz linkages can be compatible within the CRISPR system if placed in the optimized position of sgRNA. The developed conjugation strategy can potentially be employed for a variety of research application. It can be used to facilitate fluorescent labeling or tagging of sgRNAs. It can also be utilized to create sgRNA libraries.[23] In our work, the bio-orthogonal conjugation strategy has been explored to examine impacts of RNA nucleobase modifications on CRISPR efficiency.

We selected several naturally occurring RNA modifications, m^1A, m^6A, s^4U, and s^2U, which are yet to be examined in the context of CRISPR experiments. Since m^1A and m^6A destabilize RNA-DNA duplex, whereas s^2U and s^4U have stabilizing effects, we set out to test correlation with the overall CRISPR efficiency.

It turns out that three s^4U or m^1A residues completely inhibit the DNA cleavage activity probably due to the resulting unstable crRNA-DNA duplex. In comparison, three m^6A significantly increase the cleavage activity, which is contradictory to its destabilization effect on RNA-DNA. Similarly, three s^2U residues, which are expected to largely enhance the duplex stability, have a slightly negative impact on the cleavage activity. Of the 14 surveyed sgRNAs, the highest nuclease activity was exhibited by the construct containing a single s^4U modification, which was also quite unexpected.

These results indicate that there might be no direct correlations between the stabilization effect and CRISPR activity. Although more systematic structural and biophysical insights are required to investigate the impacts of these modifications on Cas9 interactions, most likely the enzyme recognition of crRNA has been changed with these modifications. In addition, for the modifications such as m^6A that can increase the DNA cleavage efficiency, the cleavage specificity or off-target effect remains to be investigated. Nonetheless, this work provides a useful platform to test more chemical modifications and identify some useful candidates to further increase both CRISPR efficiency and precision.

Authors' Contributions

A.H. carried out chemical synthesis of RNA phosphoramidites and SPS of RNA containing m^1A and m^6A modifications. A.H. performed *in vitro* CRISPR experiments. Y.Y.Z. carried out SPS of RNA containing s^2U and s^4U modifications. Y.Y.Z. performed in-cell CRISPR experiments and flow cytometry. M.R. and J.S. conceptualized the project, and they provided student supervision and

funding for the project. M.R. and J.S. wrote the manuscript with input from all authors. All authors approved the final manuscript.

Author Disclosure Statement

There are no conflicts to declare.

Funding Information

The authors gratefully acknowledge financial support by the National Institutes of Health of the United States (Grant R21HG012257 to M.R.) and the National Science Foundation (Grant CHE-1664577 to M.R.; Grants CHE-1845486 to J.S.). This work was also supported, in part, by the National Institutes of Health of the United States Grant R15GM12811501.

Supplementary Material

Supplementary Data
Supplementary Figure S1
Supplementary Figure S2
Supplementary Figure S3
Supplementary Figure S4
Supplementary Figure S5
Supplementary Figure S6
Supplementary Figure S7
Supplementary Figure S8
Supplementary Figure S9
Supplementary Figure S10
Supplementary Figure S11
Supplementary Figure S12
Supplementary Figure S13
Supplementary Figure S14
Supplementary Figure S15
Supplementary Table S1

References

1. Jinek M, Jiang F, Taylor DW, et al. Structures of Cas9 endonucleases reveal RNA-mediated conformational activation. Science 2014;343(6176):1247997; doi: 10.1126/science.1247997
2. Nishimasu H, Ran FA, Hsu PD, et al. Crystal structure of Cas9 in complex with guide RNA and target DNA. Cell 2014;156(5):935–949; doi: 10.1016/j.cell.2014.02.001
3. Wang T, Wei JJ, Sabatini DM, et al. Genetic screens in human cells using the CRISPR-Cas9 system. Science 2014;343(6166):80–84; doi: 10.1126/science.1246981
4. Gaudelli NM, Komor AC, Rees HA, et al. Programmable base editing of T to G C in genomic DNA without DNA cleavage. Nature 2017;551(7681):464–471; doi: 10.1038/nature24644
5. Cameron P, Coons MM, Klompe SE, et al. Harnessing type I CRISPR–Cas systems for genome engineering in human cells. Nat Biotechnol 2019;37(12):1471–1477; doi: 10.1038/s41587-019-0310-0
6. Finn JD, Smith AR, Patel MC, et al. A single administration of CRISPR/Cas9 lipid nanoparticles achieves robust and persistent in vivo genome editing. Cell Rep 2018;22(9):2227–2235; doi: 10.1016/j.celrep.2018.02.014
7. Maeder ML, Stefanidakis M, Wilson CJ, et al. Development of a gene-editing approach to restore vision loss in Leber congenital amaurosis type 10. Nat Med 2019;25(2):229–233; doi: 10.1038/s41591-018-0327-9
8. Frangoul H, Altshuler D, Cappellini MD, et al. CRISPR-Cas9 gene editing for sickle cell disease and β-thalassemia. N Engl J Med 2021;384(3):252–260; doi: 10.1056/nejmoa2031054
9. Lacey SF, Fraietta JA. First trial of CRISPR-edited T cells in lung cancer. Trends Mol Med 2020;26(8):713–715; doi: 10.1016/j.molmed.2020.06.001
10. Stadtmauer EA, Fraietta JA, Davis MM, et al. CRISPR-engineered T cells in patients with refractory cancer. Science 2020;367(6481):eaba7365; doi: 10.1126/science.aba7365
11. Lu Y, Xue J, Deng T, et al. Safety and feasibility of CRISPR-edited T cells in patients with refractory non-small-cell lung cancer. Nat Med 2020;26(5):732–740; doi: 10.1038/s41591-020-0840-5
12. Ledford H. CRISPR treatment inserted directly into the body for the first time. Nature 2020;579(7797):185; doi: 10.1038/d41586-020-00655-8.
13. Maxwell T. Abstracts. OFID 2021:8(Suppl 1):S633.
14. Adams D, Gonzalez-Duarte A, O'Riordan WD, et al. Patisiran, an RNAi therapeutic, for hereditary transthyretin amyloidosis. N Engl J Med 2018;379(1):11–21; doi: 10.1056/nejmoa1716153
15. Jackson LA, Anderson EJ, Rouphael NG, et al. An MRNA vaccine against SARS-CoV-2—Preliminary report. N Engl J Med 2020;383(20):1920–1931; doi: 10.1056/nejmoa2022483
16. Polack FP, Thomas SJ, Kitchin N, et al. Safety and efficacy of the BNT162b2 MRNA Covid-19 vaccine. N Engl J Med 2020;383(27):2603–2615; doi: 10.1056/nejmoa2034577
17. Balwani M, Sardh E, Ventura P, et al. Phase 3 trial of RNAi therapeutic Givosiran for acute intermittent porphyria. N Engl J Med 2020;382(24):2289–2301; doi: 10.1056/nejmoa1913147
18. Ryan DE, Taussig D, Steinfeld I, et al. Improving CRISPR-Cas specificity with chemical modifications in single-guide RNAs. Nucleic Acids Res 2018;46(2):792–803; doi: 10.1093/nar/gkx1199
19. O'Reilly D, Kartje ZJ, Ageely EA, et al. Extensive CRISPR RNA modification reveals chemical compatibility and structure-activity relationships for Cas9 biochemical activity. Nucleic Acids Res 2019;47(2):546–558; doi: 10.1093/nar/gky1214
20. Yin H, Song CQ, Suresh S, et al. Partial DNA-guided Cas9 enables genome editing with reduced off-target activity. Nat Chem Biol 2018;14(3):311–316; doi: 10.1038/nchembio.2559
21. Mir A, Alterman JF, Hassler MR, et al. Heavily and fully modified RNAs guide efficient SpyCas9-mediated genome editing. Nat Commun 2018;9(1):2641; doi: 10.1038/s41467-018-05073-z
22. McCown PJ, Ruszkowska A, Kunkler CN, et al. Naturally occurring modified ribonucleosides. Wiley Interdiscip Rev RNA 2020;11(5):e1595; doi: 10.1002/wrna.1595
23. Taemaitree L, Shivalingam A, El-Sagheer AH, et al. An artificial triazole backbone linkage provides a split-and-click strategy to bioactive chemically modified CRISPR sgRNA. Nat Commun 2019;10(1):1610; doi: 10.1038/s41467-019-09600-4
24. Jewett JC, Bertozzi CR. Cu-free click cycloaddition reactions in chemical biology. Chem Soc Rev 2010;39(4):1272; doi: 10.1039/b901970g
25. He M, Wu X, Mao S, et al. Bio-orthogonal chemistry enables solid phase synthesis and HPLC and gel-free purification of long RNA oligonucleotides. Chem Commun 2021;57(35):4263–4266; doi: 10.1039/D1CC00096A
26. Wu K, He M, Khan I, et al. Bio-orthogonal chemistry-based method for fluorescent labelling of ribosomal RNA in live mammalian cells. Chem Commun 2019;55(70):10456–10459; doi: 10.1039/C9CC05346H
27. Agustin E, Asare Okai PN, Khan I, et al. A fast click–slow release strategy towards the HPLC-free synthesis of RNA. Chem Commun 2016;52(7):1405–1408; doi: 10.1039/C5CC05392G
28. Chen Z, Devi G, Arif A, et al. Tetrazine-ligated CRISPR sgRNAs for efficient genome editing. ACS Chem Biol 2022;17(5):1045–1050; doi: 10.1021/acschembio.2c00116
29. Santner T, Hartl M, Bister K, et al. Efficient access to 3′-terminal azide-modified RNA for inverse click-labeling patterns. Bioconjug Chem 2014;25(1):188–195; doi: 10.1021/bc400513z
30. Jin S, Miduturu CV, McKinney DC, et al. Synthesis of amine- and thiol-modified nucleoside phosphoramidites for site-specific introduction of biophysical probes into RNA. J Org Chem 2005;70(11):4284–4299; doi: 10.1021/jo050061l
31. Mejia Oneto JM, Khan I, Seebald L, et al. In vivo bioorthogonal chemistry enables local hydrogel and systemic pro-drug to treat soft tissue sarcoma. ACS Cent Sci 2016;2(7):476–482; doi: 10.1021/acscentsci.6b00150
32. Karver MR, Weissleder R, Hilderbrand SA. Synthesis and evaluation of a series of 1,2,4,5-tetrazines for bioorthogonal conjugation. Bioconjug Chem 2011;22(11):2263–2270; doi: 10.1021/bc200295y
33. Schoch J, Staudt M, Samanta A, et al. Site-specific one-pot dual labeling of DNA by orthogonal cycloaddition chemistry. Bioconjug Chem 2012;23(7):1382–1386; doi: 10.1021/bc300181n

34. Iwasaki RS, Ozdilek BA, Garst AD, et al. Small molecule regulated sgRNAs enable control of genome editing in *E. coli* by Cas9. Nat Commun 2020;11(1):1394; doi: 10.1038/s41467-020-15226-8
35. Safra M, Sas-Chen A, Nir R, et al. The M1A landscape on cytosolic and mitochondrial MRNA at single-base resolution. Nature 2017;551(7679):251–255; doi: 10.1038/nature24456
36. Dominissini D, Nachtergaele S, Moshitch-Moshkovitz S, et al. The dynamic N1-methyladenosine methylome in eukaryotic messenger RNA. Nature 2016;530(7591):441–446; doi: 10.1038/nature16998
37. Zhou H, Rauch S, Dai Q, et al. Evolution of a reverse transcriptase to map N1-methyladenosine in human messenger RNA. Nat Methods 2019;16(12):1281–1288; doi: 10.1038/s41592-019-0550-4
38. Li X, Xiong X, Wang K, et al. Transcriptome-wide mapping reveals reversible and dynamic N1-methyladenosine methylome. Nat Chem Biol 2016;12(5):311–316; doi: 10.1038/nchembio.2040
39. Du H, Zhao Y, He J, et al. YTHDF2 destabilizes M6A-containing RNA through direct recruitment of the CCR4-NOT deadenylase complex. Nat Commun 2016;7(1):12626; doi: 10.1038/ncomms12626
40. Zhou J, Wan J, Gao X, et al. Dynamic M6A MRNA methylation directs translational control of heat shock response. Nature 2015;526(7574):591–594; doi: 10.1038/nature15377
41. Dominissini D, Moshitch-Moshkovitz S, Schwartz S, et al. Topology of the human and mouse M6A RNA methylomes revealed by M6A-Seq. Nature 2012;485(7397):201–206; doi: 10.1038/nature11112
42. Edupuganti RR, Geiger S, Lindeboom RGH, et al. N6-methyladenosine (M6A) recruits and repels proteins to regulate mRNA homeostasis. Nat Struct Mol Biol 2017;24(10):870–878; doi: 10.1038/nsmb.3462
43. Agris PF. Bringing order to translation: The contributions of transfer RNA anticodon-domain modifications. EMBO Rep 2008;9(7):629–635; doi: 10.1038/embor.2008.104
44. Duechler M, Leszczyńska G, Sochacka E, et al. Nucleoside modifications in the regulation of gene expression: Focus on tRNA. Cell Mol Life Sci 2016;73(16):3075–3095; doi: 10.1007/s00018-016-2217-y
45. Kumar R. Synthesis and studies on the effect of 2-thiouridine and 4-thiouridine on sugar conformation and RNA duplex stability. Nucleic Acids Res 1997;25(6):1272–1280; doi: 10.1093/nar/25.6.1272
46. Sheng J, Larsen A, Heuberger BD, et al. Crystal structure studies of RNA duplexes containing S2U:A and S2U:U base pairs. J Am Chem Soc 2014;136(39):13916–13924; doi: 10.1021/ja508015a
47. Roost C, Lynch SR, Batista PJ, et al. Structure and thermodynamics of N^6-methyladenosine in RNA: A spring-loaded base modification. J Am Chem Soc 2015;137(5):2107–2115; doi: 10.1021/ja513080v
48. Testa SM, Disney MD, Turner DH, et al. Thermodynamics of RNA-RNA duplexes with 2- or 4-thiouridines: Implications for antisense design and targeting a group I intron. Biochemistry 1999;38(50):16655–16662; doi: 10.1021/bi991187d
49. Jiang F, Doudna JA. CRISPR–Cas9 structures and mechanisms. Annu Rev Biophys 2017;46(1):505–529; doi: 10.1146/annurev-biophys-062215-010822
50. Sternberg SH, LaFrance B, Kaplan M, et al. Conformational control of DNA target cleavage by CRISPR–Cas9. Nature 2015;527(7576):110–113; doi: 10.1038/nature15544
51. Chen JS, Dagdas YS, Kleinstiver BP, et al. Enhanced proofreading governs CRISPR–Cas9 targeting accuracy. Nature 2017;550(7676):407–410; doi: 10.1038/nature24268
52. Kleinstiver BP, Pattanayak V, Prew MS, et al. High-fidelity CRISPR–Cas9 nucleases with no detectable genome-wide off-target effects. Nature 2016;529(7587):490–495; doi: 10.1038/nature16526
53. Slaymaker IM, Gao L, Zetsche B, et al. Rationally engineered Cas9 nucleases with improved specificity. Science 2016;351(6268):84–88; doi: 10.1126/science.aad5227
54. Riesenberg S, Helmbrecht N, Kanis P, et al. Improved GRNA secondary structures allow editing of target sites resistant to CRISPR-Cas9 cleavage. Nat Commun 2022;13(1):489; doi: 10.1038/s41467-022-28137-7
55. Yin H, Song C-Q, Suresh S, et al. Structure-guided chemical modification of guide RNA enables potent non-viral in vivo genome editing. Nat Biotechnol 2017;35(12):1179–1187; doi: 10.1038/nbt.4005
56. Rueda FO, Bista M, Newton MD, et al. Mapping the sugar dependency for rational generation of a DNA-RNA hybrid-guided Cas9 endonuclease. Nat Commun 2017;8(1):1610; doi: 10.1038/s41467-017-01732-9
57. Hendel A, Bak RO, Clark JT, et al. Chemically modified guide RNAs enhance CRISPR-Cas genome editing in human primary cells. Nat Biotechnol 2015;33(9):985–989; doi: 10.1038/nbt.3290
58. Rahdar M, McMahon MA, Prakash TP, et al. Synthetic CRISPR RNA-Cas9–guided genome editing in human cells. Proc Natl Acad Sci U S A 2015;112(51):E7110–E7117; doi: 10.1073/pnas.1520883112

Received: June 21, 2022
Accepted: September 26, 2022
Online Publication Date: November 15, 2022